

- 2, 1976); R. Zallen, *The Physics of Amorphous Solids* (Wiley, New York, 1983).
- H. Williams, F. J. Turner, C. M. Gilbert, *Petrography* (Freeman, San Francisco, 1954); R. B. Sosman, *The Phases of Silica* (Rutgers Univ. Press, New Brunswick, NJ, 1965); A. Spry, *Metamorphic Textures* (Pergamon, New York, 1969).
 - Polycrystalline samples of AlPO_4 berlinite were loaded in a gasketed Mao-Bell-type diamond cell. The starting material was a fragment from the single crystal used by Jayaraman *et al.* (8), part of which was ground to a grain size less than $3 \mu\text{m}$. Pressure was determined using the ruby fluorescence technique [H. K. Mao, P. M. Bell, J. W. Shaner, D. J. Steinberg, *J. Appl. Phys.* **49**, 3276 (1978)].
 - X-ray diffraction at pressure was carried out with monochromatized $\text{Mo K}\alpha$ radiation from a rotating-anode generator, with the pattern being collected on film in a Debye-Scherrer geometry; see E. Knittle and R. Jeanloz, *Science* **223**, 53 (1984); *ibid.* **235**, 668 (1987). For the x-ray diffraction runs at high pressure, $\sim 10\%$ by volume Au powder (99.99% purity, grain size less than $5 \mu\text{m}$, obtained from Alpha Ventron Corp., Danvers, MA) was mixed into the sample. This served as a calibration standard for the diffraction intensities of the sample, and no other pressure medium was used.
 - Samples of AlPO_4 (8% by weight) mixed in CsI were compressed between anvils of type II diamond. Absorption spectra were collected between 300 cm^{-1} and 3700 cm^{-1} (4 cm^{-1} resolution) with a Bomem DA 3.02 Fourier transform spectrometer equipped with a liquid helium-cooled Ge:Cu detector; see Q. Williams and R. Jeanloz, *Science* **239**, 902 (1988).
 - The difference between infrared absorption spectra of crystals and corresponding glasses is illustrated in and discussed by R. Zallen [in (2)]. The interpretation of the infrared absorption spectrum of AlPO_4 berlinite is discussed by E. Z. Aldridge, V. C. Farmer, B. D. Mitchell, W. A. Mitchell, *J. Appl. Chem.* **13**, 17 (1963). The spectrum of our sample at ambient conditions is in good agreement with theirs.
 - A. Jayaraman, D. L. Wood, R. G. Maines, Sr., *Phys. Rev. B* **35**, 8316 (1987).
 - S. M. Sharma and S. K. Sikka, *Pramana*, in press.
 - R. J. Hemley *et al.*, *Nature* **334**, 52 (1988).
 - The Pauling bond strengths for the Al-O, Si-O, and P-O bonds are 0.75, 1.0, and 1.25, respectively. Further discussion of the relation between bond strength and pressure-induced amorphization is given in M. B. Kruger and R. Jeanloz, in preparation.
 - Y. Fujii *et al.*, *J. Phys. C* **18**, 789 (1985); S. Sugai, *ibid.*, p. 799; F. E. A. Melo *et al.*, *Phys. Rev. B* **35**, 3633 (1987); H. Sankaran *et al.*, *ibid.* **38**, 170 (1988); M. B. Kruger *et al.*, *J. Chem. Phys.* **91**, 5910 (1989); C. Meade and R. Jeanloz, *Geophys. Res. Lett.*, in press.
 - O. Mishima *et al.*, *Nature* **310**, 393 (1984); R. J. Hemley *et al.*, *ibid.* **338**, 638 (1989); Q. Williams and R. Jeanloz, *ibid.*, p. 413; Q. Williams *et al.*, *J. Geophys. Res.*, in press.
 - The single crystal samples were compressed as described above (4), except that a hydrous 4:1 mixture of methanol:ethanol was used as a pressure medium; see G. J. Piermarini, S. Block, J. D. Barnett, *J. Appl. Phys.* **44**, 5377 (1973). This pressure medium becomes nonhydrostatic at pressures above $\sim 14 \text{ GPa}$.
 - The apparent birefringence is the observed optical retardation divided by the sample thickness. Thus, δ depends on the crystallographic orientation of the sample. It was determined by means of white, cross-polarized transmitted light (16).
 - F. D. Bloss, *An Introduction to the Methods of Optical Crystallography* (Holt, Rinehart and Winston, New York, 1961).
 - R. Jeanloz *et al.*, *Science* **197**, 457 (1977); R. Jeanloz, *J. Geophys. Res.* **85**, 3163 (1980).
 - The magnitude of shear stress varies from one experimental run to the next and is quantified by measuring the pressure gradients across the sample [see C. Meade and R. Jeanloz, *J. Geophys. Res.* **93**, 3261 (1988); *ibid.*, p. 3270; *Science* **241**, 1072 (1988)].
 - Q. Williams and R. Jeanloz, *Nature* **338**, 413 (1989).
 - C. Meade and R. Jeanloz, *Rev. Sci. Instr.*, in press.
 - We thank A. Jayaraman for providing the sample material used in this study, C. Meade for help in digitizing the x-ray films, and Q. Williams, C. Meade, M. Pasternak, B. O'Neill, and E. Stolper for helpful comments on the manuscript. This work was supported by Exxon Research and Engineering Co. and the National Science Foundation.

10 April 1990; accepted 20 June 1990

Water and Solutions at Negative Pressure: Raman Spectroscopic Study to -80 Megapascals

J. L. GREEN, D. J. DURBEN, G. H. WOLF, C. A. ANGELL

Microscopic inclusions of aqueous fluids trapped in interstices in quartz and other crystals provide novel systems for the deliberate study of liquids under tension. Liquids under tension should differ in interesting ways from those at ambient pressure or compressed liquids because attractive, rather than repulsive, forces should dominate their behavior. Static tensions in excess of 100 megapascals (~ 1000 atmospheres) have been obtained reproducibly. Video-recorded observations of the final liquid rupture process, coupled with extrapolations of data at positive pressure, suggest that the homogeneous vapor nucleation point was reached in two of the cases studied. Raman spectra of the fluids at -80 megapascals show that an isothermal volume stretch of ~ 5 percent by volume has only a weak effect on the spectral features and is similar to the effect of isobaric heating.

INTEREST IN THE PROPERTIES OF WATER under tension (that is, at negative pressure) has been stimulated by the conjecture of Speedy (1) that the much investigated divergences of thermodynamic properties and relaxation times in supercooled water (2) are related to comparable divergences in properties of superheated water (3) through a continuous line of mechanical instabilities. For this relation to be possible, the spinodal limit to liquid superheating and stretching, which is predictable for any liquid from reasonable equations of state (EoS) (1, 4-6), must behave anoma-

lously in the negative pressure regime in the case of water. The spinodal line for water, obtained from the National Bureau of Standards (NBS) EoS (5) where $(\partial P/\partial V)_T = 0$, is shown against the phase diagram for water in Fig. 1. (This contrasts with "normal" behavior predicted by the van der Waals EoS in which the spinodal line moves to ever more negative pressures with decreasing temperature.) Speedy's much simpler (two-parameter) EoS, derived with the assumption of a spinodal limit to the liquid and fit to EoS data from 0° to 100°C and 0 to 100 MPa, yields a somewhat larger tensile limit (dashed line in Fig. 1).

Figure 1 differs from the standard textbook phase diagram for water by inclusion

of a gray area for metastable liquid states, most of which falls in the negative pressure domain. At the boundaries of this region, fluctuation correlation lengths diverge, as at the critical point (4, 6), and the metastable liquid become mechanically unstable. Anomalous behavior, comparable to the divergence of compressibility, viscosity, and other properties of supercooled water [where an origin in spinodal fluctuations has

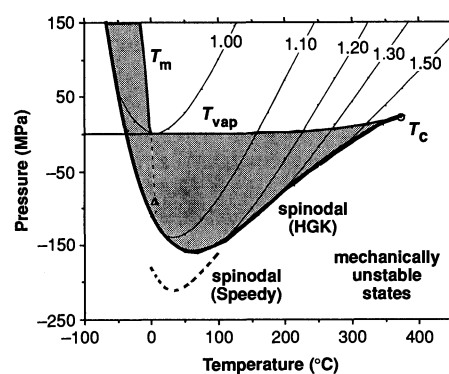


Fig. 1. Phase diagram for water showing thermodynamically stable (open) and metastable (shaded) regions. Thin lines are isochores (specific volumes are marked). The spinodal boundary according to the NBS EoS is given as a thick curve commencing at the critical temperature, T_c , whereas the part of the spinodal assessed by Speedy with a (more reliable) two-parameter equation is shown as a thick dashed line. The tension estimated by Roedder for a fluorite inclusion from the observed ice melting point elevation (1) is marked as a triangle on the extrapolated melting line, T_m .

Department of Chemistry, Arizona State University, Tempe, AZ 85287.

been suggested (1, 2)] should therefore be observable anywhere in the vicinity of the spinodal. Thus successful penetration into the negative pressure regime is a great challenge to the experimentalist.

Attempts to study water under tension have been sporadic (7) and have in most cases been limited to pressure ranges far below the theoretical limit because of the difficulty of suppressing heterogeneous nucleation of vapor bubbles. Even Speedy and collaborators (8–10), who applied one of the small-sample techniques successful in supercooled water research to investigate water under tension, failed by a large margin to realize the tensile limit of approximately 200 MPa that is predicted by EoS analyses (1, 7) and supported by detailed molecular dynamics simulations (11). One case in which the limit seems to have been closely approached, however, was reported by Roedder (12), who used naturally occurring microscopic inclusions of water in fluorite to observe ice melting at +6.5°C. This observation, as Roedder pointed out, requires that the ice-water system be under a tension of ~95 MPa, which is 80 or 60% of the spinodal limit for water at this temperature, depending on whether the NBS or the Speedy EoS is used as reference (see Fig. 1).

Roedder's observation suggests that the route to detailed exploration of the negative pressure regime for liquids (13) is via the study of synthetic liquid inclusions in suitable host materials. The preparation of such samples achieves the essential requirements for suppression of heterogeneous nucleation (2) (that is, microfiltration, microsequestration, and pyrolysis).

We tested this idea using water-in-quartz inclusions to show that tensions in excess of 100 MPa may be sustained in favorable cases. To characterize the water under these conditions (and simultaneously to assess its purity), we extended the earlier Raman study of water under 20-MPa tension (9) to the new microscopic samples, using micro-Raman techniques developed for diamond-anvil-cell high-pressure studies (14).

We have studied inclusions in two samples, one synthesized by hydrothermal crystal growth methods and one by autoclaving quench-fissured quartz crystals in the presence of excess water (15). In the first case the inclusion is trapped and isolated by the growing crystals, and in the second case it is formed as the fissures heal, trapping the aqueous phase at a density that depends on the temperature and pressure of the autoclave.

Sample 1 was a fragment of a large quartz crystal hydrothermally synthesized several years ago at Bell Labs and much studied by inclusion scientists because of its transparen-

cy. Although the included liquid is a saline or hydroxide solution (see below), the sample was adopted for study because two of the inclusions formed parallel columns (see Fig. 2A) that are microscopic (~5 μm by 70 μm) versions of the tubular samples used originally by Berthelot (16) in the first systematic study of water under tension. We followed Berthelot's procedure and obtained much larger tensions than he was able to generate.

Sample 2, in which the inclusion is quasi-spherical (Fig. 2B), was synthesized at ~1000°C and 1.5 GPa by Rovetta (17) using initially pure water and the fissure-healing technique (15). When the inclusion has no bubble (see below), the density of the trapped aqueous phase is much higher than in Sample 1. Both ambient temperature Raman spectra (see below) and melting point studies indicate that the Sample 2 fluid is also a solution. The Raman spectra of the trapped fluids in the two samples are, unexpectedly, almost identical. Comparison of these spectra with those of NaCl solutions (18) suggests that the concentration of the impurity is equivalent to 0.80 molal NaCl, consistent with our microthermometrically observed 3.0°C depression of the melting point of the fluid (0.81 molal).

The origin of the contamination [which is commonly found in fissure-synthesized inclusions (17)] is uncertain although scavenging of alkali ions Li⁺ and Na⁺ from charge compensating sites near impurity Al³⁺ centers in the quartz is suspected from microprobe analysis (17). Some leaching of the metal container is also indicated by a brownish tinge to the quartz sample and a strong fluorescence background in the Raman spectra. That the contamination is due to

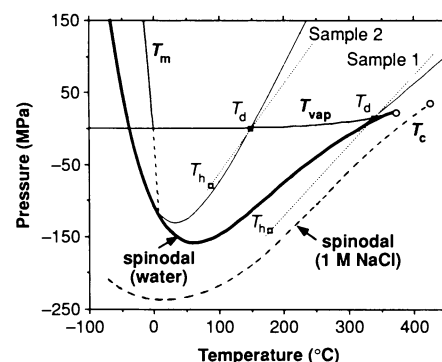


Fig. 3. Spinodal for water showing isochores for pure water (solid lines) and 1 molal NaCl solution (dotted lines) that pass through the T_d values of Samples 1 and 2. For pure water, the isochores are extrapolated to the spinodal on the basis of the HGK EoS. For the NaCl solutions, an estimation of the spinodal position is given, on the basis of the known critical point, the critical isochore (which fixes the initial spinodal slope), and the temperature of maximum density relative to water (which fixes where the spinodal extremum must occur).

alkali electrolytes could not be unambiguously determined from our spectroscopic measurements. The possibility of significant silica leaching into the fluid phase was ruled out by the absence of Si-OH bands in the Raman spectra. Contamination by HCO₃⁻ could not be evaluated spectroscopically because quartz has a Raman line located at exactly the same frequency as the most intense HCO₃⁻ line. The possibility, suggested by the similarity of spectra of samples of quite different origin, that the spectra are of pure water that is structurally and thermodynamically altered by the close proximity of SiO₂ walls, has been considered but discounted. Wall effects, which may depress the

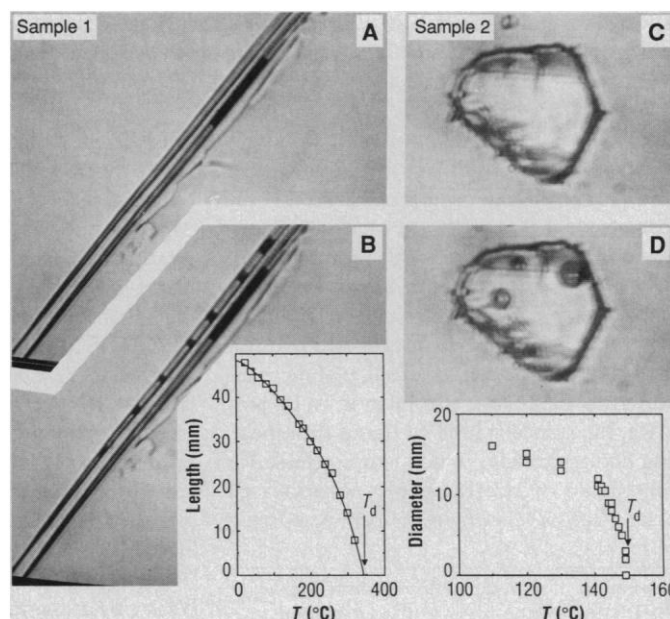


Fig. 2. Photographs from video recording of Samples 1 (A and B) and 2 (C and D) before (A and C), and shortly after (B and D), fluid cavitation under tension. Much bubble coalescence had already occurred when the photo was taken (the lower tubule in (A) had already cavitated). Inserts show behavior of the bubble on heating and define the bubble disappearance temperature T_d ; hence, also the appropriate isochore that is followed on cooling.

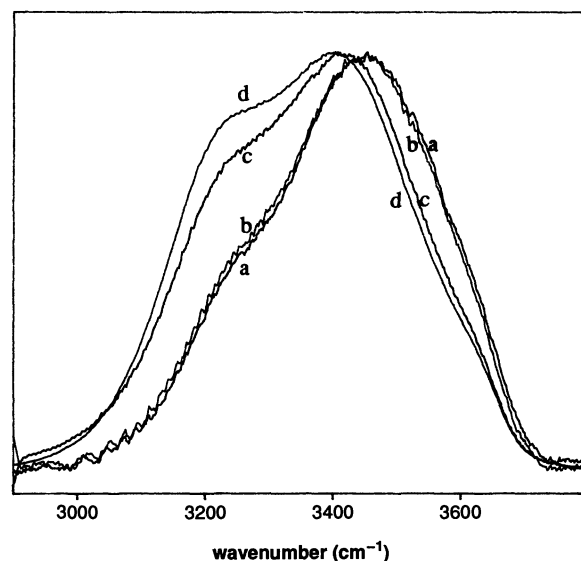
density maximum in water (19), only occur for dimensions of $<2 \mu\text{m}$, and even then the melting point remains $\sim 0^\circ\text{C}$ (19).

At room temperature, aqueous inclusions contain vapor bubbles that occupy 20 to 50% of the total volume, depending on conditions of formation (12). In order to produce tension in the liquid, the bubble must first be eliminated by thermal expansion. During heating, the pressure follows the equilibrium vapor pressure curve for as long as the bubble remains up to the well-defined temperature of bubble disappearance, T_d (see Fig. 2). Above T_d the pressure must rise more rapidly, and it follows an isochore fixed by the liquid EoS (5, 6) and T_d (Fig. 3). Isochores for both pure water (5, 6) and 1 molal NaCl solutions (20) that pass through the T_d for the bubbles in each sample (upper tubule of Sample 1) are shown in Fig. 3. The pressure variation above T_d is almost linear; therefore, the extrapolation into the negative pressure region is fairly unambiguous. Because quartz is almost incompressible and nonexpansive relative to water, the deviation of the actual sample pressure from the true isochoric path shown in Fig. 3 is small [$<10\%$ correction (21)].

On cooling, the (corrected) isochore must be followed until the bubble reappears. In the case of the lower of the Sample 1 tubules, the bubble reappeared at a temperature only 35 K below T_d , where tension is small (see below). The early rupture was presumably because of some heterogeneous nucleation site on the quartz, in that the bubble always reappeared at the same site in repeated experiments. By contrast, the upper tubule of Sample 1, and the Sample 2 inclusion, could be cooled far below their respective T_d values. In Sample 1 the liquid in the inclusion remained intact down to 179°C , 161° below T_d , where it ruptured catastrophically to produce microscopic bubbles throughout the liquid (Fig. 2B). This behavior would be expected in a homogeneous nucleation process; therefore, we have denoted the temperature of rupture as T_h (3, 5, 6).

We can estimate the pressure at which the rupture occurred by moving down the appropriate isochore to T_h . For the inclusion in Sample 1 there is considerable uncertainty in this pressure because isochores intersect the spinodal line tangentially, and low-density isochores with T_d values near the critical point (374°C for water) are only slightly subparallel to the spinodal line (Fig. 1). In this high temperature region, a small displacement of the spinodal line or deviation in the isochore slope can have a large effect on the projected spinodal pressure, P_s , at the stability limit of an isochore. For the upper

Fig. 4. Parallel-polarized Raman spectra of stretched and normal water at 92°C ; curve a, uncavitated Sample 1 at $\sim -80 \text{ MPa}$; curve b, cavitated Sample 1 at its own vapor pressure; curve c is the spectrum of the cavitated sample at 25°C for comparison with curve d, the spectrum for pure bulk water at 25°C (indicating the presence of impurities in the inclusion).



tubule in Sample 1, the observed cavitation temperature is far below the spinodal for a pure water sample with the same T_d . However, using a linear extrapolation of an isochore constructed from pressure-volume-temperature data for a 1 molal NaCl solution (20) (which has a considerably higher critical temperature, 423°C) we estimate that the rupture occurred at a pressure of $-140 \pm 20 \text{ MPa}$ [corrected to -136 MPa (21)]. Before this inclusion could be studied by Raman spectroscopy, it began to behave irreproducibly both with respect to T_d and T_h , and the cavitation phenomenon lost the catastrophic character observed initially.

In the case of the Sample 2 inclusion (Fig. 2B), T_d is only 149°C , implying an isochore of much greater density and slope than for Sample 1. The rupture temperature in this case was 87°C , a value that is 62°C below T_d and corresponds to a pressure of -82 MPa [corrected to -74 MPa (21)]. Unlike the Sample 1 inclusion, which lost its ability to stretch, T_d and T_h for the Sample 2 inclusion were reproducible within $\pm 0.5^\circ\text{C}$ for many cycles. Because the cavitation process always had the same dramatic character, indicative of homogeneous nucleation, the relatively low pressure compared with the theoretical limit for a 1 molal aqueous solution, which should exceed that for pure water on this isochore, is surprising.

The volume strain, ξ , at T_h can be obtained from values of the molar volume V_m of 1 molal NaCl aqueous solution (20) on the equilibrium liquid-vapor line, at T_d and T_h [$V(T_d)$ and $V(T_h)$, respectively], according to

$$\xi = \frac{V_0}{V_0 - V_{\text{bubble}}} - 1 = V(T_d)/V(T_h) - 1$$

V_0 is the volume of the filled vesicle and V_{bubble} is the volume of the vapor bubble

that forms at T_h . The calculated volume strain for the inclusion in Sample 2 was 5% at 87°C . In the Sample 1 inclusion, the volume strain is approximately 35%. Such values are much greater than the 0.4% observed in earlier experiments on bulk o-terphenyl (13).

Because extrapolations of multiparameter EoS beyond their domains of observation can be misleading, it is instructive to use the above stretching fraction with Speedy's two parameter EoS (1) for pure water to estimate the tension at T_h . Accordingly, a tension of -105 MPa is obtained for sample 2, which is larger than our earlier estimate (partly because of the effect of the salt content).

We obtained Raman spectra of the Sample 2 inclusion at T_d , and at 20°C intervals down to the point of rupture at T_h , using a micro-Raman triple spectrometer (ISA S3000) and an intensified diode array detector (Princeton Instruments). The 488-nm line of a continuous wave Ar^+ laser, with beam aligned parallel to the c axis of the quartz crystal, was focused to a spot of approximately $5 \mu\text{m}$ in diameter within the vesicle with the use of a long working distance $\times 50$ microscope objective (Mitutoyo SL50). The Raman signal was collected in a 180° backscattering geometry, through the same microscope objective, and then polarization-analyzed. The power level at the sample was approximately 50 mW, sufficiently low to avoid temperature perturbations. Spectra of good quality could be obtained with collection times of 2 min. A relatively strong fluorescence from the quartz sample interfered with the Raman spectra but could be minimized with spatial filtering. The remaining fluorescence interference was subtracted in our spectra. The lowest temperature spectrum of the uncavitated sample was taken at 92°C , only slightly

above the rupture temperature of 87°C, and corresponds to a pressure of about -80 MPa.

Comparison of the parallel-polarized Raman spectra of the Sample 2 inclusion in the fundamental -O-H stretching region at 92°C both before and after rupture (Fig. 4) reveals that, despite the ~5% difference in density between the cavitated and stretched samples, their Raman spectra are nearly indistinguishable. This result was not unexpected because both Raman spectra and infrared spectra are known to respond only weakly to positive pressure changes (22). Some minor differences in the Raman spectra of the cavitated and uncavitated liquids at 92°C are discernible. For the sample under tension, there is a small loss in intensity of the lower frequency shoulder and a small positive shift of the main band peak relative to the cavitated sample. These differences indicate that, in the temperature range of our study, isothermal stretching has qualitatively the same effect on structure as isobaric thermal expansion (23). Computer simulation studies of the stretched state of water (9) suggest that this may not be the case at lower temperatures. It should be possible to study this interesting aspect on samples prepared to maximize the tension without provoking cavitation. The relations in Fig. 1 suggest that one should be able to pass solutions through the temperature of maximum density (the temperature of maximum tension in a constant volume experiment) which should be reached at about -150 MPa.

Our observations show that physico-chemical studies of liquids are possible in a pressure-temperature regime in which the physical properties are dominated by the attractive component of the intermolecular potential. The low-frequency vibrational modes, the compressibility, and the structural relaxation times of water should be much more sensitive to tension than are the high-frequency vibrational spectra, especially as the spinodal limit is approached. The challenge will now be to exploit microscopic Brillouin scattering techniques developed for ultrahigh-pressure studies in diamond cells (24) to explore more fully the properties of water and other liquids in this new and interesting regime.

REFERENCES AND NOTES

1. R. J. Speedy, *J. Phys. Chem.* **86**, 982 (1982).
2. C. A. Angell, *J. Chem. Phys.* **65**, 851 (1976).
3. C. A. Angell, *Annu. Rev. Phys. Chem.* **79**, 3921 (1983).
4. L. Landau and I. M. Lifschitz, *Statistical Physics* (Addison-Wesley, London, 1958), p. 264.
5. L. Haar, J. Gallagher, G. S. Kell, National Bureau of Standards-National Research Council Steam Tables (McGraw-Hill, New York, 1985).

6. C. A. Angell, W. J. Sichina, M. Oguni, *J. Phys. Chem.* **86**, 998 (1982).
7. D. H. Trevena, *Contemp. Phys.* **17**, 109 (1976); *Am. J. Phys.* **47**, 341 (1979).
8. R. J. Henderson and R. J. Speedy, *J. Phys. E* **13**, 778 (1980).
9. J. L. Green, A. R. Lacey, M. G. Sceats, S. J. Henderson, R. J. Speedy, *J. Phys. Chem.* **91**, 1684 (1987).
10. S. J. Henderson and R. J. Speedy, *ibid.*, p. 3062.
11. A. Geiger, *Proceedings of the NATO Advanced Study Institute on Hydrogen Bonded Liquids*, J. C. Dore and J. Teixeira, Eds. (Plenum, New York, in press).
12. E. Roedder, *Science* **155**, 1413 (1967); *Fluid Inclusions*, P. H. Ribbe, Ed. (*Rev. Mineral.*, vol. 12, Mineralogical Society of America, Washington, DC, 1984).
13. C. A. Angell and Q. Zheng, *Phys. Rev. Rap. Commun.* **39**, 8784 (1989).
14. G. H. Wolf *et al.*, *J. Chem. Phys.*, in press.
15. S. M. Sternar and R. J. Bodnar, *Geochim. Cosmochim. Acta* **48**, 2659 (1984).
16. M. Berthelot, *Ann. Chem. Ser. 3* **30**, 232 (1850).
17. M. R. Rovetta, J. D. Blacic, R. L. Hervig, J. R. Holloway, *J. Geophys. Res.* **94**, 5840 (1989); M. R. Rovetta, personal communication.
18. T. P. Mernagh and A. R. Wilde, *Geochim. Cosmochim. Acta* **53**, 765 (1989).
19. J. H. Shufle and M. Venogoplan, *J. Geophys. Res.* **72**, 3271 (1967); A. N. Savitskii, *Russ. Colloid. J.* **30**, 199 (1968).
20. G. C. Kennedy, *Econ. Geol.* **45**, 629 (1950); G. J. Wasserburg, H. C. Heard, R. C. Newton, *Am. J. Sci.* **260**, 501 (1962); J. L. Haas, Jr., *U.S. Geol. Surv. Bull.* **1421** (1976), data in part C by R. W. Potter II and D. L. Brown.
21. On the basis of compressibility and thermal expansivity data for quartz, we estimate that the ratio of the volume at T_d to the volume at the cavitation temperature, T_c , of the uncavitated fluid will be 1.011 and 1.005 for Samples 1 and 2, respectively. This effect results in approximate reductions of 3% and 10% of the tensions of cavitation indicated on Fig. 3 for Samples 1 and 2, respectively.
22. G. E. Walrafen, *J. Solution Chem.* **2**, 159 (1973); V. Rodgers, thesis, Purdue University, West Lafayette, IN (1981).
23. J. R. Scherer, M. K. Go, S. Kint, *J. Phys. Chem.* **78**, 1304 (1974).
24. A. Polian and M. Grimsditch, *Phys. Rev. B* **27**, 6409 (1983); L. Oliver, C. Herbst, G. H. Wolf, in preparation.
25. This work has been supported by the National Science Foundation (grants NSF-DMR-CHE8304887 and NSF-EAR8657437) and the Shell Foundation fellowship program.

12 February 1990; accepted 8 May 1990

Direct Cloning of Human Transcripts with HnRNA from Hybrid Cell Lines

LAURA CORBO,* JULIE A. MALEY, DAVID L. NELSON, C. THOMAS CASKEY†

A library of human-derived complementary DNA from a human-hamster hybrid cell line containing the Xq24-qter region has been constructed. Complementary DNA synthesis was primed from heterogeneous nuclear (hn) RNA by oligonucleotides derived from conserved regions of human *Alu* repeats. At least 80% of these cloned sequences were of human origin, providing an enrichment of at least two orders of magnitude. Two clones, one containing a fragment of the primary transcript of the human hypoxanthine-guanine phosphoribosyltransferase (HPRT) gene at Xq26 and another recognizing a family of human genes mapping to two regions of Xq24-qter, were characterized. Additional hncDNA clones mapped to a variety of sites in the Xq24-qter region, demonstrating the isolation of many transcriptionally active loci. These clones provide probes for identification of genetic loci on the terminal region of the X chromosome long arm, which is the location of a number of inherited disorders.

THE ABILITY TO PURIFY HUMAN transcripts from specific regions of the genome would greatly facilitate its characterization (1). The Xq24-qter region of the human X chromosome encodes a minimum of 25 genetic disorders whose genes are unknown (2). This region is therefore particularly attractive for the investigation of its gene content. We have isolated transcribed sequences from the human

Xq24-qter region using a hybrid cell line, X3000-11.1 (3), which retains this human chromosomal region in a hamster background. This approach takes advantage of hybrid cell lines to reduce the complexity of the genomic region under study and exploits the presence of human *Alu* repetitive elements in introns and 3'-untranslated regions of human transcripts.

HnRNA, extracted from purified nuclei of X3000-11.1 and RJK88 (hamster parent of X3000-11.1), was used as template to synthesize first-strand hncDNA. Two oligonucleotides, TC-65 and 517, from the same *Alu* region but in opposite orientations, have been shown to bind specifically to human *Alu* sequences in a hamster or mouse background (4). They were used separately to prime the synthesis of human hncDNA

L. Corbo, J. A. Maley and D. L. Nelson, Institute for Molecular Genetics, Baylor College of Medicine, Houston, TX 77030.

C. T. Caskey, Institute for Molecular Genetics and Howard Hughes Medical Institute, Baylor College of Medicine, Houston, TX 77030.

*On leave of absence from Institute of Experimental and Clinical Oncology, Medical School, University of Reggio Calabria, Catanzaro, Italy.

†To whom correspondence should be addressed.